ORIGINAL PAPER

A glassy carbon electrode modified with porous gold nanosheets for simultaneous determination of dopamine and acetaminophen

Qian-Li Zhang · Jin-Xia Feng · Ai-Jun Wang · Jie Wei ·
Zhang-Ying Lv · Jiu-Ju Feng

Abstract Porous gold nanosheets modified glassy carbon electrode (GCE) was facilely prepared by one-step electrodeposition, using *N*-methylimidazole as a growth-directing agent. The porous gold nanosheets modified GCE was characterized by scanning electron microscopy, transmission electron microscopy, and X-ray diffraction spectroscopy. The modified electrode displayed improved sensitivity for individual and simultaneous differential pulse voltammetric determination of dopamine (DA; at 180 mV) and acetaminophen (AC; at 450 mV vs. Ag/AgCl) even in the presence of ascorbic acid. The oxidation peak currents linearly increased with the concentrations of DA and AC in the ranges from 2.0 to 298.0 μM and 3.0 to 320.0 μM, respectively, and the detection limits are 0.28 μM for DA and 0.23 μM for AC. The relative standard deviations ($n=20$) are 1.5 % for DA and 0.4 % for AC.

Keywords Electrodeposition · Porous gold nanosheets · Dopamine · Acetaminophen

Introduction

Dopamine (DA) is an important electroactive neurotransmitter, which provides communicating link between neurons [1].

Q.-L. Zhang · J.-X. Feng · J. Wei
School of Chemistry and Biological Engineering, Suzhou University of Science and Technology, Suzhou 215009, China
e-mail: jjfeng@zjnu.cn

A.-J. Wang · Z.-Y. Lv · J.-J. Feng
College of Geography and Environmental Science, College of Chemistry and Life Science, Zhejiang Normal University, Jinhua 321004, China

A.-J. Wang
e-mail: ajwang@zjnu.cn

As a medicine, its deficiency or sufficiency would cause brain disorder disease such as Parkinson's disease and schizophrenia [2, 3]. As a result, DA is usually used to treat the depression for its function of transmission the mood of fun and excitement. Thus, the detection of DA is a key point in biomedical chemistry, diagnostic and pathological research.

However, the assay of DA in body fluid is seriously affected by many coexisted interfering compounds such as acetaminophen (AC) and ascorbic acid (AA) [4]. Specifically, AC is an antipyretic and analgesic drug used for relief of fever, headaches, and other minor aches and pains [5]. Besides, it has wide applications in osteoarthritis and ovarian cancer therapy [6]. Nevertheless, its surplus will induce toxic metabolite accumulation, causing acute hepatic necrosis [7]. Additionally, AA is a vital vitamin in human diet and very popular in foodstuffs for its antioxidant property, which can be applied to prevent and treat common cold, mental illness, infertility, cancer, and AIDS [8, 9].

It is essential for selective and/or simultaneous detection of DA and AC in the presence of AA, because AA, DA, and AC usually coexist in real biological samples [4]. Up to now, several methods have been developed for detection of DA and AC, including capillary electrophoresis [10], chromatography [11], chemiluminescence [12], spectrophotometric [13], and electrochemical method [14, 15]. Among them, electrochemical methods are widely used, owing to their intrinsic advantages such as rapid response, high sensitivity, easy operation, and low cost.

The electrochemical oxidation peaks of AA, DA, and AC are usually overlapped on a bare glassy carbon electrode (GCE), leading to poor selectivity and reproducibility [16]. For simultaneous determination of DA and AC, several modified electrodes have been constructed with multiwall carbon nanotubes [17], nano-TiO_2/polymer [18], polypyrrole/ aszophloxine/Au [19], and Fe_3O_4@Au-S-Fc/GS-chitosan [4] as electrode modifiers. It is still a challenge for their

electrochemically selective or simultaneous determination without the interference with each other.

Gold nanostructures become extremely popular in a wide range recently, due to their optical, electrical, and chemical properties [20, 21]. For instance, gold nanoparticles have been widely used in surface plasmonics [22], surface-enhanced Raman scattering (SERS) [23], chemical and biological sensing [24].

We prepared porous gold nanosheets modified GCE by one-step electrodeposition, which is simple, feasible, facile, cost-effective, and environmental benign, along with high purity and uniform structures of the deposits [25]. The electrocatalytic properties of the modified GCE were examined by selective and simultaneous detection of DA and AC as model systems.

Experimental

Materials

HAuCl$_4$, N-methylimidazole, AA, DA, and AC were purchased from Shanghai Aladdin Chemical Reagent Company (Shanghai, China, www.aladdin-reagent.com). All the other reagents were of analytical grade and used without further purification. The aqueous solutions were prepared with twice-distilled water (18.2 MΩ, 1~2 μS cm^{-1}) throughout the whole experiments.

Preparation of porous gold nanosheets modified GCE

The preparation process for porous gold nanosheets modified GCE was described in our previous work [26], denoted as porous gold nanosheets/GCE. Briefly, the electrodeposition process was performed by applying a constant potential of −0.4 V on a clean GCE for 600 s in 0.5 M H$_2$SO$_4$ containing 10 mM HAuCl$_4$ and 1.25 M N-methylimdazole. For comparison, gold nanoparticles were prepared on a GCE in the absence of N-methylimdazole, while other conditions were kept constant, which is named as gold nanoparticles/GCE. Finally, the electrodes were thoroughly washed with water and dried in air.

Electrochemical experiments were performed on a CHI 660D electrochemical workstation (Chenhua Instrument Shanghai Co., Ltd, China, www.chinstr.com). A conventional three-electrode system was used, where the Ag/AgCl electrode, platinum wire, and bare or modified GCE were used as the reference, counter, and working electrodes, respectively. Differential pulse voltammograms (DPVs) were recorded by using the following settings: step potential of 4 mV, amplitude of 50 mV, pulse width of 0.2 s, sample width of 0.02 s, and pulse period of 0.5 s. All measurements were performed at 25 °C, if not stated otherwise.

Characterization

The morphology and structures of the deposits were characterized by field emission scanning electron microscopy (SEM, JSM-7,500 F, www.jeol.co.jp/en.com) and a JEM-2,100 F transmission electron microscope (TEM) operating at an accelerating voltage of 200 KV (www.jeol.co.jp/en.com), respectively. The modified GCE was sonicated in ethanol after electrodeposition to obtain a homogeneous suspension, and then a drop of the solution was deposited on a Cu grid for TEM observation. X–ray diffraction

Fig. 1 SEM image (a), TEM images (b, c), and XRD patterns (d) of porous gold nanosheets. Inset shows the corresponding SAED patterns
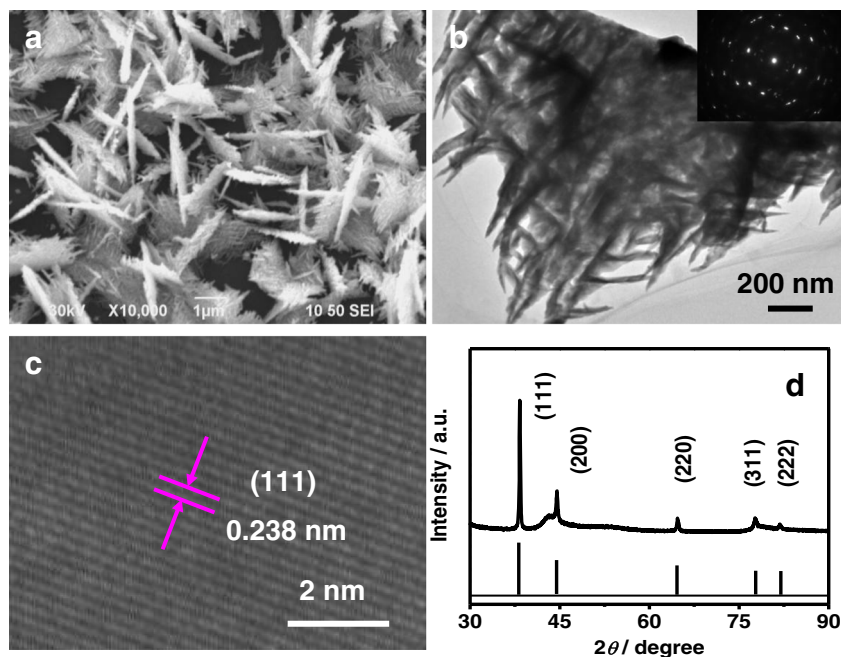
(XRD) spectra were recorded on a Rigaku Dmax–2000 diffractometer (www.rigaku.com) with a Cu Kα radiation source (λ=0.15418 nm), in which porous gold nanosheets were directly electrodeposited on the surface of a glassy carbon sheet (1.0 cm×1.0 cm).

Results and discussion

Characterization of porous gold nanosheets

One-step electrodeposition was applied for preparation of porous gold nanosheets, which was constructed in 0.5 M H_2SO_4 containing 10 mM $HAuCl_4$ and 1.25 M N-methylimdazole at −0.4 V for 600 s, owing to selective adsorption, π-π interactions, and steric hindrance of N-methylimidazole [26]. Fig. 1 shows SEM and TEM images of representative porous gold nanosheets, as well as their corresponding XRD patterns. Clearly, porous gold nanosheets are assembled by numerous tiny multi-scaled dendritic sub-branches, which are vertically standing on the electrode surface with uniform size and distribution (Fig. 1a). Low- and high-resolution TEM images (Fig. 1b and c) show their crystal orientation and growth directions. The thin tip of the tiny sub-branch from a single gold nanosheet displays clear lattice fringes with the same orientation and lattice spacing. The d value is measured to be 0.238 nm corresponding to the (111) planes of the face-centered cubic (fcc) gold crystals [27]. It indicates that porous gold nanosheets are preferentially growing along the (111) directions. Moreover, the selected area electron diffraction (SAED) of the thin branch tips (inset in Fig.1b) shows a typical diffraction spots, indicating single-crystal nature of porous gold nanosheets. Fig. 1d shows the XRD pattern of porous gold nanosheets. The representative peaks at 38.3°, 44.6°, 64.7°, 77.6°, and 81.8° are assigned to
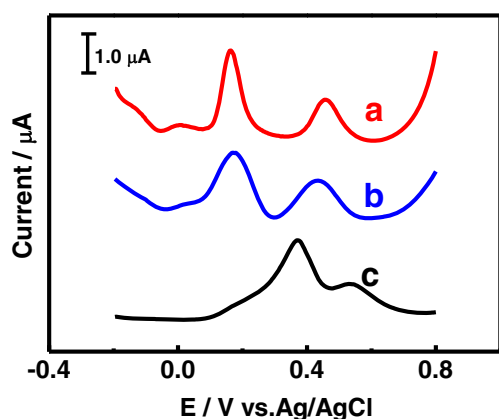

Fig. 3 Effects of pH on the peak currents (**a**) and separation of the peak potentials (**b**) for the oxidation of 0.5 mM AA, 0.1 mM DA, and 0.1 mM AC in 0.1 M phosphate solutions

the (111), (200), (220), (311), and (222) planes of the fcc Au (JCPDS 04–0784), respectively [28]. Furthermore, compared with other planes, the intensity of Au (111) planes is particularly sharp and strong. These phenomena further verify that the aggregations of gold nanocrystals are preferentially growing along the (111) directions [29].

Electrochemical behaviors

The performance of porous gold nanosheets/GCE for simultaneous determination of AA, DA, and AC is evaluated by differential pulse voltammograms (DPVs) in 0.1 M phosphate solutions (pH 7.0) containing 0.2 mM AA, 0.1 mM DA, and 0.1 mM AC (Fig. 2). As can be seen, the oxidation peaks of AA, DA, and AC are emerged at 9, 162, and 457 mV, respectively, which are well separated from each other. Impressively,

Fig. 2 DPVs of 0.2 mM AA, 0.1 mM DA, and 0.1 mM AC in 0.1 M phosphate solutions (pH 7.0) at porous gold nanosheets/GCE (curve a), gold nanoparticles/GCE (curve b), and bare GCE (curve c)
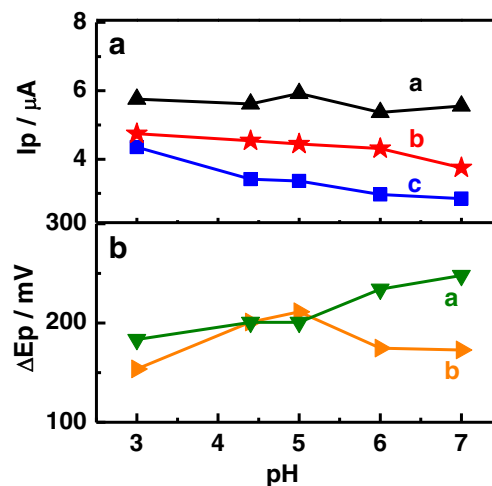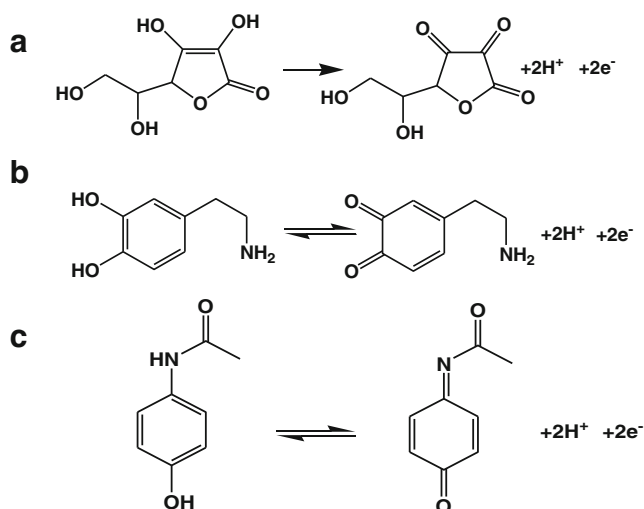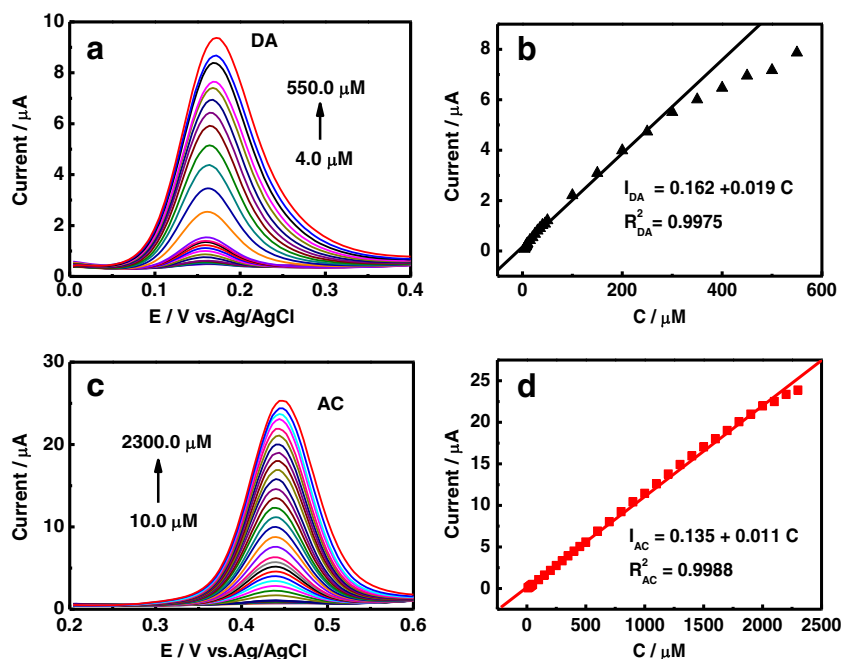

Fig. 4 Electrocatalytic oxidation of (**a**) AA, (**b**) DA, and (**c**) AC on porous gold nanosheets/GCE

Fig. 5 DPVs of porous gold
nanosheets/GCE in 0.1 M
phosphate solutions (pH 7.0) with
different concentrations of DA (**a**)
and AC (**c**). The corresponding
linear relationship between the
current and concentration of DA
(**b**) and AC (**d**)

the oxidization current is very small for AA, indicating its
poor sensitivity. Similar observation is obtained for AA oxi-
dation on gold nanoparticles/GCE. Moreover, the oxidation
peaks of DA and AC are stronger and sharper, compared with
those on gold nanoparticles/GCE. Additionally, on bare GCE,
there are two oxidation peaks from AA and DA completely
overlapped at 372 mV, and AC oxidation peak is detected at
546 mV, which is partially overlapped with those of AA and
DA. Therefore, it is most practical and reasonable for

simultaneous determination of DA and AC in the presence
of AA on porous gold nanosheets/GCE.

Effects of pH

The pH effects on electrochemical oxidation of AA, DA, and
AC are investigated on porous gold nanosheets/GCE by dif-
ferential pulse voltammograms (DPVs) in 0.1 M phosphate
buffer solutions in the pH range from 3.0 to 7.0 (Fig. 3). The

Fig. 6 DPVs of porous gold
nanosheets/GCE in 0.1 M
phosphate solutions (pH 7.0)
containing 0.1 mM AC in the
presence of different concentrations
of DA (**a**) and AC (**c**). The linear
relationship between the peak
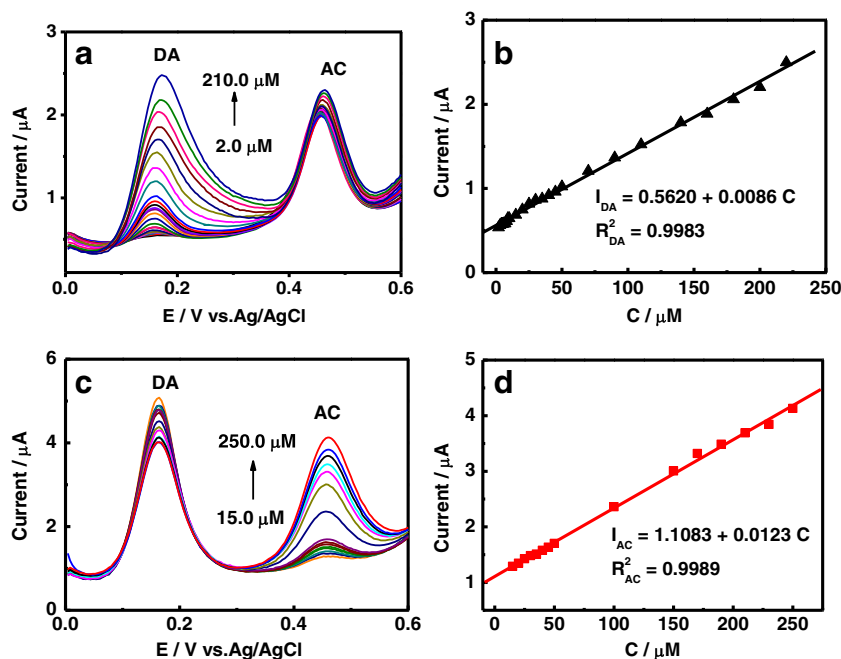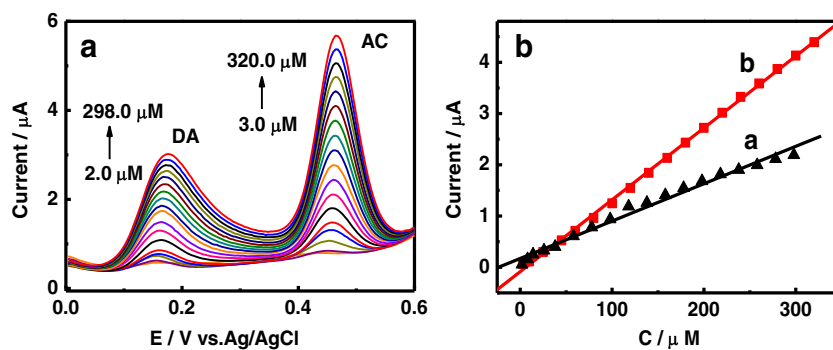current and the concentration of
DA (**b**) and AC (**d**)

Fig. 7 (**a**) DPVs of porous gold nanosheets/GCE in 0.1 M phosphate solutions (pH 7.0) containing different concentrations of DA and AC. (**b**) The corresponding linear relationship between the peak current and DA (curve a)/AC (curve b) concentrations

oxidation potentials are found negatively shifted with the increased pH values from 3.0 to 7.0. It confirm that protons are involved in the electrode reaction process. Fig. 4 shows the corresponding electrocatalytic oxidation mechanism of AA (a), DA (b), and AC (c), respectively. The results are consistent with the previous reports [18, 19, 30].

Figure 3a shows the effects of pH values on the peak currents of AA (curve b) and AC (curve c). The corresponding peak currents slightly decrease with the increase of pH values. However, the peak currents of DA increase with pH values when the pH is below 5.0, while their peak currents (curve a) are almost constant when the pH is above 5.0.

Besides, Fig. 3b displays the effects of pH on the separation of the two oxidation peak potentials (ΔE_{pa}) between DA and AA (curve b)/AC (curve a). In the pH range of 3.0~7.0, the ΔE_{pa} between DA and AA achieves the maximum at pH 5.0; while the ΔE_{pa} between AC and DA achieves the maximum at pH 7.0. As can be observed, AA, DA, and AC can be completely separated on porous gold nanosheets/GCE. However, the responses of AA gradually become weak during the detection process. This is due to weak adsorptions of DA and AC on gold nanostructures [31], compared with those of AA, inducing the detection of AA with very low sensitivity under the same conditions (Fig. 2). Therefore, simultaneous detection of DA and AC is possible, without any interference of AA. Considering well separation of DA and AC, along with

physiological environment, pH 7.0 was chosen for the following study.

Simultaneous determination of DA and AC

Figure 5 illustrates DPVs of DA (Fig. 5a, b) and AC (Fig. 5c, d) with different concentrations at porous gold nanosheets/GCE, respectively. As shown in Fig. 5b, the oxidation peak currents of DA increase linearly with the concentration from 4.0 to 298.0 μM (R^2=0.9975) with a detection limit of 0.12 μM (S/N=3). Similarly, the oxidation peak currents are also positively proportional to AC in the concentration range of 10.0~2300.0 μM (R^2=0.9988), with a detection limit of 0.25 μM (S/N=3). Moreover, the corresponding slopes are estimated to be 0.019 and 0.011 μA μM^{-1} for DA and AC, respectively.

Figure 6 and 7 show DPVs of DA and AC on porous gold nanosheets/GCE for their selective detection. As shown in Fig. 6, with the increase of DA concentrations from 2.0 to 210.0 μM, the anodic peak currents linearly increase in the presence of 0.1 mM AC. Similar trend is observed by increasing AC from 15.0 to 250.0 μM in the presence of 0.1 mM DA. The sensitivities of DA and AC are calculated to be 0.009 and 0.012 μA μM^{-1}, respectively, with the detection limit (S/N=3) of 0.69 μM for DA and 1.27 μM for AC.

Figure 7 shows DPVs for simultaneous detection of DA and AC with different concentrations. The anodic peak

Table 1 Comparison of different modified electrodes for simultaneous detection of DA and AC

Electrode	Linear range (μM)		Detection limit (μM)		Ref.
	DA	AC	DA	AC	
Fe$_3$O$_4$@Au-S-Fc/GS-chitosan/GCE	0.5–50	0.4–32	0.08	0.01	[4]
f-MWCNTs/GCE	3–200	3–300	0.80	0.60	[17]
PAY/nano-TiO$_2$/GCE	12–120	12–120	1.0	2.0	[18]
SWCNT/CCE	0.4–150	0.2–100	0.22	0.12	[32]
FEPA-GR-CS/GCE	2–135	0.3–80	0.30	0.05	[33]
gold nanosheets/GCE	2–298	3–320	0.28	0.23	This work

currents show the linear increase with DA from 2.0 to 298.0 μM (I_{DA} (μA)=0.1389+0.0074 C (μM), R^2=0.9952) and AC from 3.0 to 320.0 μM (I_{AC} (μA)=–0.0862+0.0140 C (μM), R^2=0.9995), respectively. From the linear equations, the sensitivities of DA and AC are found to be 0.007 μA μM^{-1} and 0.014 μA μM^{-1}, respectively, with the detection limits of 0.28 μM for DA and 0.23 μM for AC. For simultaneous determination of DA and AC, Table 1 shows the comparison of the electrochemical performances of porous gold nanosheets/GCE with other modified electrodes in the literature [4, 17, 18, 32, 33]. Porous gold nanosheets/GCE exhibits the widest linear range and comparable detection sensitivity.

It is worth noting that the sensitivities of porous gold nanosheets/GCE are almost identical for AC detection in the absence and presence of DA, and vice versa. It indicates that the oxidation processes of DA and AC are independent in our system. Therefore, independent or simultaneous assays of the two targets are not interfered with each other [34]. The relative standard deviations (RSDs) of the peak currents for 20 successive measurements are 1.5 % for DA and 0.4 % for AC with the concentrations of 0.1 mM, showing the improved reproducibility of porous gold nanosheets/GCE. The enhanced reproducibility reveals porous gold nanosheets/GCE is not subject to surface fouling by the oxidation product.

Interference study

Possible interference of some other substances for detection of DA and AC is also studied by recording DPVs in 0.1 M phosphate solutions (pH 7.0) in the presence of 0.1 mM DA and AC. The criterion for interference was a relative error of less than±5 %. The common inorganic ions such as 100-fold Na^+, K^+, NH_4^+, Cl^-, NO_3^-, CH_3COO^- and CO_3^{2-} have no interference with AC and DA detection. What's more, several organic compounds such as 50-fold glucose, lactose, sucrose, lysine, aspartic acid, and urea, 25-fold cysteine and glutathione, 10-fold ascorbic acid hardly cause interference. Additionally, proteins should be firstly removed from the bio-fluids samples, which are easily fouling the electrodes.

The repeatability and stability of detection

The repeatability of the electrode was also investigated, where the RSDs were 2.1 % for AC (n=5) and 2.3 % for DA (n=5) using the same electrode. The RSDs for different electrodes prepared independently were 3.3 % for AC and 3.5 % for DA (n=5), respectively. The stability of porous gold nanosheets/GCE is investigated by recording DPVs in 0.1 M phosphate solutions containing 0.1 mM DA and AC. The amperometric responses were 92.7 % for AC and 93.6 % for DA of their initial values after a storage period of 4 weeks, revealing long-term stability of the modified electrode.

Conclusions

A simple and facile one-step electrodeposition method was developed for preparation of porous gold nanosheets/GCE. The resultant electrodes show improved sensitivity, reproducibility, anti-interference, and stability for simultaneous determination of DA and AC. Moreover, independent or simultaneous detection of DA and AC is not interfered with each other, because the sensitivity of porous gold nanosheets/GCE toward AC is almost unchanged in the absence and presence of DA, and vice versa. Meanwhile, porous gold nanosheets/GCE displays strong anti-interference ability for AA, because the oxidation of AA can be well separated from those of DA and AC.

References

1. Mahshid S, Li C, Mahshid SS, Askari M, Dolati A, Yang L, Luo S, Cai Q (2011) Sensitive determination of dopamine in the presence of uric acid and ascorbic acid using TiO_2 nanotubes modified with Pd, Pt and Au nanoparticles. Analyst 136:2322
2. Cui R, Wang X, Zhang G, Wang C (2011) Simultaneous determination of dopamine, ascorbic acid, and uric acid using helical carbon nanotubes modified electrode. Sens Actuators B 161:1139
3. Ojani R, Raoof J-B, Zarei E, Azizi S, Abrishamkar M (2012) A novel sensor for simultaneous determination of dopamine and uric acid using a new MFI-type zeolite prepared by microwave-assisted synthesis. Monatsh Chem 143:7
4. Liu M, Chen Q, Lai C, Zhang Y, Deng J, Li H, Yao S (2013) A double signal amplification platform for ultrasensitive and simultaneous detection of ascorbic acid, dopamine, uric acid and acetaminophen based on a nanocomposite of ferrocene thiolate stabilized Fe_3O_4@ Au nanoparticles with graphene sheet. Biosens Bioelectron 48:75
5. Madrakian T, Haghshenas E, Afkhami A (2013) Simultaneous determination of tyrosine, acetaminophen and ascorbic acid using gold nanoparticles/multiwalled carbon nanotube/glassy carbon electrode by differential pulse voltammetric method. Sens Actuators B 193:451
6. Bui M-PN, Li CA, Han KN, Pham X-H, Seong GH (2012) Determination of acetaminophen by electrochemical co-deposition of glutamic acid and gold nanoparticles. Sens Actuators B 174:318
7. Nasirizadeh N, Shekari Z, Zare HR, Ardakani SA, Ahmar H (2013) Developing a sensor for the simultaneous determination of dopamine, acetaminophen and tryptophan in pharmaceutical samples using a multi-walled carbon nanotube and oxadiazole modified glassy carbon electrode. J Braz Chem Soc 24:1846
8. Xu T-Q, Zhang Q-L, Zheng J-N, Lv Z-Y, Wei J, Wang A-J, Feng J-J (2014) Simultaneous determination of dopamine and uric acid in the presence of ascorbic acid using Pt nanoparticles supported on reduced graphene oxide. Electrochim Acta 115:109
9. Zheng X, Zhou X, Ji X, Lin R, Lin W (2013) Simultaneous determination of ascorbic acid, dopamine and uric acid using poly(4-aminobutyric acid) modified glassy carbon electrode. Sens Actuators B 178:359

10. Li X, Pan J, Yang F, Feng J, Mo J, Chen Z (2011) Simple amperometric detector for microchip capillary electrophoresis, and its application to the analysis of dopamine and catechol. Microchim Acta 174:123

11. Zhang C, Li J, Xu L, Shi Z-G (2012) Fast immobilized liposome chromatography based on penetrable silica microspheres for screening and analysis of permeable compounds. J Chromatogr A 1233:78

12. Haslag CS, Richter MM (2011) Electrogenerated chemiluminescence quenching of Ru(bpy)$_3^{2+}$ (bpy=2,2′-bipyridine) in the presence of acetaminophen, salicylic acid and their metabolites. J Lumin 132:636

13. Moghadam MR, Dadfarnia S, Shabani AMH, Shahbazikhah P (2011) Chemometric-assisted kinetic-spectrophotometric method for simultaneous determination of ascorbic acid, uric acid, and dopamine. Anal Biochem 410:289

14. Lakshmi D, Bossi A, Whitcombe MJ, Chianella I, Fowler SA, Subrahmanyam S, Piletska EV, Piletsky SA (2009) Electrochemical sensor for catechol and dopamine based on a catalytic molecularly imprinted polymer-conducting polymer hybrid recognition element. Anal Chem 81:3576

15. Yin H, Shang K, Meng X, Ai S (2011) Voltammetric sensing of paracetamol, dopamine and 4-aminophenol at a glassy carbon electrode coated with gold nanoparticles and an organophillic layered double hydroxide. Microchim Acta 175:39

16. Thiagarajan S, Tsai T-H, Chen S-M (2009) Easy modification of glassy carbon electrode for simultaneous determination of ascorbic acid, dopamine and uric acid. Biosens Bioelectron 24:2712

17. Alothman ZA, Bukhari N, Wabaidur SM, Haider S (2010) Simultaneous electrochemical determination of dopamine and acetaminophen using multiwall carbon nanotubes modified glassy carbon electrode. Sens Actuators B 146:314

18. Kumar SA, Tang C-F, Chen S-M (2008) Electroanalytical determination of acetaminophen using nano-TiO$_2$/polymer coated electrode in the presence of dopamine. Talanta 76:997

19. Gholivand MB, Amiri M (2012) Simultaneous detection of dopamine and acetaminophen by modified gold electrode with polypyrrole/aszophloxine film. J Electroanal Chem 676:53

20. Dreaden EC, Alkilany AM, Huang X, Murphy CJ, El-Sayed MA (2012) The golden age: gold nanoparticles for biomedicine. Chem Soc Rev 41:2740

21. Rosi NL, Mirkin CA (2005) Nanostructures in biodiagnostics. Chem Rev 105:1547

22. Lee Y-J, Schade NB, Sun L, Fan JA, Bae DR, Mariscal MM, Lee G, Capasso F, Sacanna S, Manoharan VN, Yi G-R (2013) Ultrasmooth, highly spherical monocrystalline gold particles for precision plasmonics. ACS Nano 7:11064

23. Wu H-L, Tsai H-R, Hung Y-T, Lao K-U, Liao C-W, Chung P-J, Huang J-S, Chen IC, Huang MH (2011) A comparative study of gold nanocubes, octahedra, and rhombic dodecahedra as highly sensitive SERS substrates. Inorg Chem 50:8106

24. Zhang Q-L, Zhou D-L, Li Y-F, Wang A-J, Qin S-F, Feng J-J (2014) Cytosine-assisted synthesis of gold nanochains and gold nanoflowers for the construction of a microperoxidase-11 based amperometric biosensor for hydrogen peroxide. Microchim Acta181:1239

25. Feng J-J, Li A-Q, Lei Z, Wang A-J (2012) Low-potential synthesis of "clean" Au nanodendrites and their high performance toward ethanol oxidation. ACS Appl Mat Interfaces 4:2570

26. Feng J-J, Lv Z-Y, Qin S-F, Li A-Q, Fei Y, Wang A-J (2013) N-methylimidazole-assisted electrodeposition of Au porous textile-like sheet arrays and its application to electrocatalysis. Electrochim Acta 102:312

27. Fang Y, Ren Y, Jiang M (2011) Co-effect of soft template and microwave irradiation on morphological control of gold nanobranches. Colloid Polym Sci 289:1769

28. Shin H-S, Hong J-Y, Huh S (2013) 2-Thiopheneacetic acid directed synthesis of Au nanorosette as an SERS-active substrate. ACS Appl Mat Interfaces 5:1429

29. Jiu J, Suganuma K, Nogi M (2011) Effect of additives on the morphology of single-crystal Au nanosheet synthesized using the polyol process. J Mater Sci 46:4964

30. Zhao Y, Gao Y, Zhan D, Liu H, Zhao Q, Kou Y, Shao Y, Li M, Zhuang Q, Zhu Z (2005) Selective detection of dopamine in the presence of ascorbic acid and uric acid by a carbon nanotubes-ionic liquid gel modified electrode. Talanta 66:51

31. Ge P-Y, Du Y, Xu J-J, Chen H-Y (2009) Selective detection of dopamine based on the unique property of gold nanofilm. J Electroanal Chem 633:182

32. Habibi B, Jahanbakhshi M, Pournaghi-Azar MH (2011) Simultaneous determination of acetaminophen and dopamine using SWCNT modified carbon-ceramic electrode by differential pulse voltammetry. Electrochim Acta 56:2888

33. Wang L, Liu M, Meng Y, Li H, Zhang Y, Yao S (2013) (4-Ferrocenylethyne) phenylamine on graphene as the signal amplificator to determinate dopamine and acetaminophen simultaneously. Chin J Chem 31: 845

34. Zare HR, Nasirizadeh N (2009) Application of hematoxylin multiwall carbon nanotube modified carbon paste electrode as a chemical sensor for simultaneous determination of dopamine and acetaminophen. Int J Electrochem Sci 4:1691